First Results of GPS Measurements Along the Lai Chau - Dien Bien Fault in North-West Vietnam

Chi Cong DUONG*, Hong-Sic YUN**, Jae-Myong CHO*** and Dong-Ha LEE****

Abstract

GPS measurements from Feb. 2002 through Mar. 2004 were used to estimate recent crustal movement across the Lai Chau - Dien Bien fault system in North-West Vietnam. Four GPS campaign data were processed and combined with appropriate constraints using automatic GAMIT/GLOBK run in order to estimate ITRF2000 coordinates, local horizontal velocity and extensive/compressive strain rates. ITRF2000 velocities are consistent with east-southeastward movement of Sundaland i.e. Indochina. Local velocities show not much left-lateral strike-slip of the fault system and derived strain rates are insignificant from zero at 95% confidence.

Keywords : Crustal deformation, GPS, Southeast Asia

1. Introduction

With about 500 km length the Lai Chau - Dien Bien fault (LC-DBF) stretches from its nearest point to Red River fault - north of Chieng Chai Village (Vietnam-China border), through Lai Chau, Dien Bien Provinces in Vietnam, to its end in Louang Phrabang Province in Laos (Lacassin et al. 1997, Holt et al. 2000, Burchfiel 2004). Its part in Vietnam is approximately 160 km long and 6-10 km wide (Fig. 1 and 2).

During Cenozoic the LC-DBF has passed two main tectonic development stages, which are characterized by right-lateral and reverse right-lateral strike-slip, and by left-lateral and normal left-lateral strike-slip mechanisms respectively. The boundary between these two stages was possibly in Pliocene (Lacassin et al, 1997; Nguyen et al, 2001). A tectonic map of the eastern part of the Tibetan plateau and adjacent areas from the late Cenozoic to recent time from Burchfiel (2004) also shows that the LC-DBF belongs to the left-lateral strike-slip faults.

There are some evidences of recent activity of the LC-DBF at a local scale: 1) Earthquakes have been occurring along the fault zone and in its adjacence, and most of them have reached magnitudes larger than 4.0 Richter (Fig. 2); 2) Sources of thermal water have become exposed on surface near the fault zone: for example, in the northwest of Muong Pon Village and Dien Bien Town; 3) The geothermal and geochemistry values of emanation (of Ra, Hg, CO_2, CH_4) show high anomalies in Lai Chau Town, Na Pheo Village, etc.; and 4) Landslides and accompanying mudflows have been occurring frequently, which sometimes lead to disasters like those in 1996 and 1997 at Muong Lay Town (Nguyen et al, 2001).

Before 2002, some geodetic results concerning the Xianshuihe-Xiaojiang fault system and the Red River fault contiguous to the LC-DBF were reported. King et al. (1997) showed the result of analysis of 2-4 year GPS data, which were consistent with the left-lateral slip of 12 ± 4 mm/yr on the Xianshuihe-Xiaojiang fault system. Analyzing GPS measurements collected in 1994, 1996, 1998 and 2000, with ties in 2001, in Yen Bai, Phu Tho, Vinh Phuc, Ha Tay Provinces in
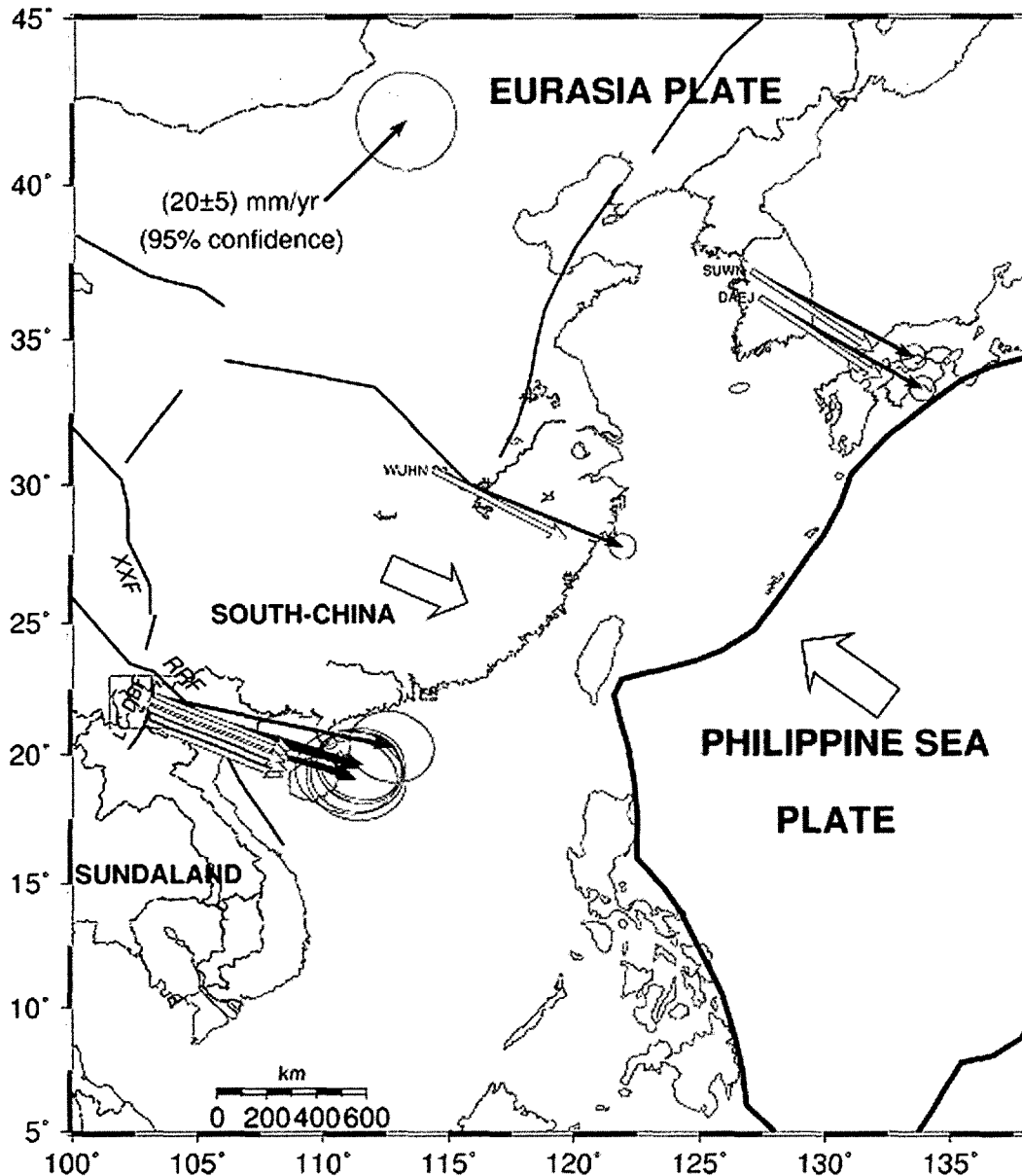
Fig. 1. Vietnam and adjacent region. Heavy lines with thickness gradually reduced show plate boundary and faults by their size; XXF: Xianshuihe-Xiaojiang Fault, RRF: Red River Fault; LC-DBF: Lai Chau - Dien Bien Fault from Lacassin et al. (1997), Holt et al. (2000), and Nguyen et al. (2001). Rectangle delimits the study area shown in Fig. 2. Black arrows with error ellipses represent our ITRF2000 velocity solution, open thin ones are from NUVEL-1A model (DeMets et al. 1994), open wide ones depict direction of movements of the Philippine Sea Plate, South-China and Sundaland blocks (Michel et al. 2000, 2001). Thin and dashed lines are rivers and international borders respectively.

Vietnam, Feigl et al. (2003) conclude that at the local scale Red River fault did not slip faster than 1 or 2 mm/yr between 1994 and 2001.

This paper shows initial three-year (2002-2004) GPS measurements and results from processing these measurements in a local-scale network spanning the LC-DBF zone in the Northwest of Vietnam. These geodetic results will give a preliminary and quantitative

assessment of recent activity of the LC-DBF for earthquake forecast and natural hazards prevention.

2. Data Precision and Estimation Strategy

Our geodetic network covers an area of 100 km x 20 km along the LC-DBF. It includes 7 stations listed by name of the main benchmark from north to south:

NGA1, DON1, HAM1, LEM1, TAU2, TAU1, TAT1. These stations are distributed regularly along the major fault (Fig. 2). Each station has at least 2 benchmarks: the main is numbered 1 and auxiliaries are numbered 2, 3, etc., except TAU1 and TAU2. Benchmarks are stainless steel cylinder pins build in bedrock where it is possible. LEM2 is the 3rd, HAM2, and TAU1 are the 4th order points belong to GPS network of Geodetic Survey of Vietnam. Their composition included concrete with porcelain mark on it.

GPS measurements were carried out 4 campaigns from February 2002 to March 2004 in almost the same (dry) season to avoid influence of local dislocation on benchmarks (Table 1).

Tie measurements between main and auxiliary benchmarks were carried out just before the beginning of the 1st and the 2nd campaigns with 1 hour session at each site and were not included in data processing.

4 TRIMBLE SSI, 1 TRIMBLE SSE receivers, COMPACT L1/L2 with Ground Plane antennas, and only 1 MICRO CENTERED L1/L2 with Ground Plane antenna for the 4th campaign were used to record GPS signals. For no concrete pillar in the network, we had to do point centering with a tripod. GPS data sampling rate of 30 sec and 6° elevation mask were set to obtain more precise upward component (Nguyen Ngoc Lau 2002a). Each session lasted about 23h 30m. RINEX transfer, and only simple quality check was run in situ after each session of field campaigns.

GPS observations were analyzed according to standard procedures (Feigl et al. 1993, King and Bock 2003, Herring 2003). *Firstly* we use GAMIT software for processing single sessions, including 5 IGS stations: NTUS in Singapore, SHAO (Shanghai) for *lf2a* experiment, WUHN (Wuhan) in China, SUWN (Suwon), and DAEJ (Daejon) in Korea. These IGS stations

Table 1. Availability of GPS observations from Feb. 2002 to Mar. 2004. Terms in brackets are experiment names in GAMIT processing

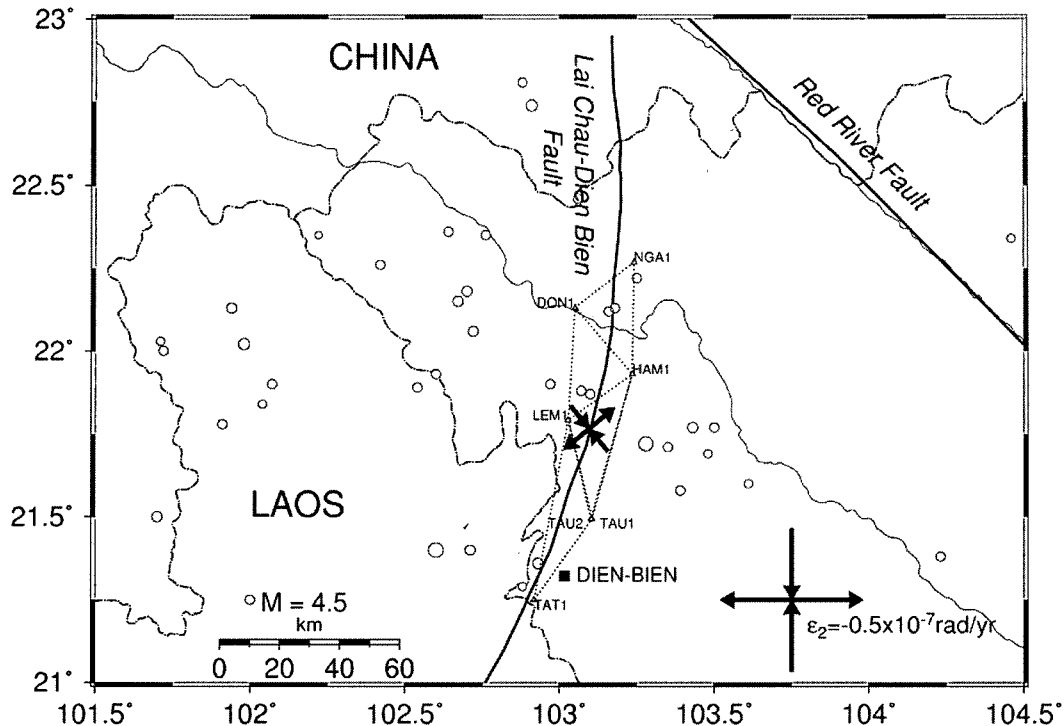|		NGA1	DON1	HAM1	LEM1	TAU1	TAU2	TAT1
2002 (lf2a)	054	x	x	x	x		x	
	055	x	x	x	x		x	
	056	x	x	x	x		x	
	057	x	x	x	x		x	
	058	x	x	x	x		x	
2002 (lf2b)	318		x			x		x
	319		x					x
	320		x	x				
	321		x	x	x			
	323			x	x			x
	324			x	x	x		
	325				x	x		
	326					x	x	x
2003 (lf03)	051	x	x	x	x		x	
	052	x	x	x	x		x	
	053	x	x	x	x		x	
	054	x	x	x	x		x	
	055	x	x	x	x		x	
2004 (lf04)	058	x	x	x	x		x	
	059	x	x	x	x		x	
	060	x	x	x	x		x	
	061	x	x	x	x		x	
	063					x	x	x
	064					x	x	x
	065					x	x	x

- 53 -

Fig. 2. GPS network with its stations (*shaded triangles*) and their names, earthquake epicenters (*shaded circles*) in a study area with magnitude M > 3.5 from the USGS (US Geological Survey) catalog (1973 - Mar. 2005), faults (*heavy lines*), rivers (*thin lines*), international borders (*dashed lines*), and the maximum extension, compression strain parameters estimated from our ITRF2000 velocity solution for the whole network

were chosen because they are situated in not so actively deforming blocks in the region (Michel et al. 2000, 2001). Their actual ITRF2000 coordinates and velocities were as ties with the global reference frame. We used IERS (International Earth Rotation and Reference Systems Service) Earth orientation parameters and updated elevation-dependent antenna phase-center models proposed by the US National Geodetic Survey (Rothacher and Mader 1996, King and Bock, 2003). GAMIT run was done by automatic processing scripts from getting navigation, precise orbit, permanent IGS station's observation files to daily or sequence of consecutive days processing. Some considerable options for every (day) session processing are as follows:

- Appropriate constraint for initial condition and non-gravitational force parameters of all satellites,
- Use of double-differenced GPS phase observations with ionospheric-free phase combination,
- Estimate station coordinates and orbital parameters,
- Estimate 13 tropospheric zenith delay parameters using default standard tropospheric models (Nguyen Ngoc Lau 2002b, King and Bock 2003),

- Use updated elevation-dependent antenna phase-center model,
- Apply models of diurnal, semi-diurnal Earth tides, pole tide, and ocean tide for the time-variable displacement in station coordinates,
- Estimate pole position, its rates, UT1, and UT1's rates with tight constraints.

Quality of daily solutions can be assessed by evaluating repeatabilities of RMS of independent baseline components about their mean value i.e. mean repeatability (Larson and Agnew 1991). Mean WRMS for orbit re-estimated, bias-free and bias-fixed daily solutions are shown for each campaign in Table 2.

There was not so much improvement from bias-free to bias-fixed solutions. Futhermore, WRMS of up components was larger than the one of horizontal components. Of the many effects on the collected GPS data, multipath and Anti-Spoofing can explain these differences.

Time of sessions for some campaigns, for example, 2002a..., was not within the UTC day. This produced a data gap of about half hour because of the reset of the receiver clock. We tried to divide such sessions

Table 2. Mean WRMS for the shortest baselines from daily solutions

Solution type (Re-estimated orbit)		Mean Repeatability (mm)		
		North	East	Up
lf2a	bias-free	1.7	3.8	13.6
	bias-fixed	**1.7**	**3.3**	**13.4**
lf2b	bias-free	1.5	3.0	4.5
	bias-fixed	**1.6**	**1.7**	**5.0**
lf03	bias-free	2.6	3.5	13.4
	bias-fixed	**2.6**	**2.9**	**13.4**
lf04	bias-free	1.6	2.6	8.0
	bias-fixed	**1.6**	**2.7**	**8.1**

into sub-sessions e.g. /055a, /055b... but it did not improve considerably the precision of estimated coordinates and baseline lengths. So we kept the default 1 UTC day sessions for daily processing. Use of antenna with ground plane could reduce not all of the sources of measurement biases. Baseline component repeatabilities versus baseline length for *lf04* campaign are shown in Fig. 3, just for illustrating. For not so many measured distances are available it had better to determine the "best fitting" line for WRMS values. From Table 2 we adopted bias-fixed solutions as a

result of GAMIT daily processing for all campaigns.

Secondly we applied Kalman filter (using GLOBK) to combine loosely constrained estimates of station coordinates and orbits with their covariances from each session. For small span network and there are not so many permanent IGS stations in adjacent area we did not combine our daily solutions with global ones available from SOPAC (Scripps Orbit and Permanent Arrays Center). Holding orientation of our network through IGS orbit and IERS Earth orientation parameters we followed the iterative process proposed by Herring (2003) to get a consistent coordinates of all stations as individual GPS network adjustment over each campaign. After time series of coordinates and baseline lengths had been checked for outliers we excluded NTUS from further velocity solutions because of large RMS of coordinates and baseline lengths associated with it. Precision of baseline length is obtained by the following formula:

$$\sigma_{Length} = \sqrt{a^2 + (bL)^2},$$

where values of a and b can be seen from Table 3, and L is the distance between benchmarks.

These values give an average relative precision of
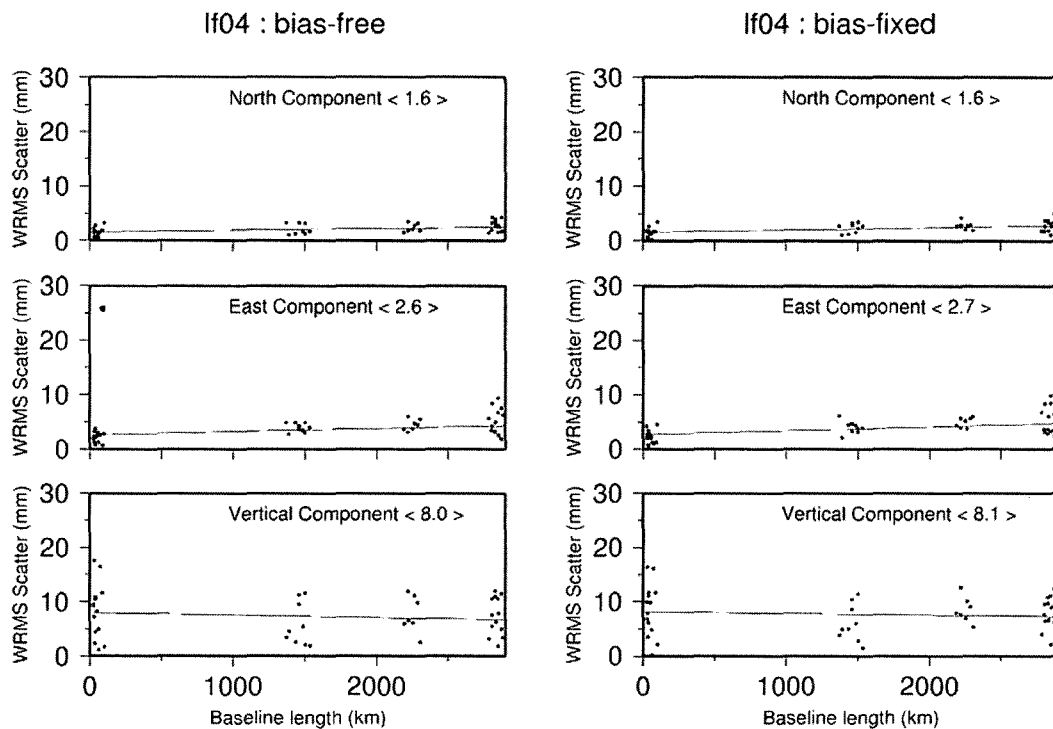
lf04 : bias-free

lf04 : bias-fixed

Fig. 3. Baseline component repeatabilities versus baseline length for *lf04* campaign. *Values in brackets* are from *Table 2. Thin line* represents the "best fitting" line

Table 3. Precision of baseline length estimated from loosely constrained combination of sessions for individual campaigns

	a (mm)	b (ppb)
1f2a	2.14	1.04
1f2b	1.50	0.95
1f03	2.79	1.71
1f04	2.16	1.54

10^{-7} for the shortest measured baseline length (~20 km) in our network.

We have also used GIPSY-OASIS II software for GPS data processing for each experiment and the results were compared with GAMIT/GLOBK results. No considerable differences found between the two results (Yun and Hwang, 2002). Therefore, we chose the GAMIT/GLOBK result for further velocity solutions.

In the *third step* we applied appropriate constraints to get reference frame for determination of horizontal velocity fields (Dong et al 1998) in a study area using GLOBK. Two kinds of velocity fields (Herring 2003) had been estimated from four sets (*1f2a*, *1f2b*, *1f03*, *1f04*) of GPS data:

1) Horizontal velocities in ITRF2000 by minimizing adjustments of ITRF2000 velocities of IGS stations used in analysis, and

2) Relative horizontal velocities between strands of the main fault with several options:
   - Assuming 3 IGS stations: WUHN, SUWN, DAEJ, with NGA1, HAM1, TAU1(2), and TAT1 locate on a single block (Michel et al. 2000, 2001; Feigl et al. 2003).
   - Same as previous but at the local scale: excluding IGS stations.
   - Minimum constraints also within a local frame: fix two (DON1, LEM1) or (NGA1, HAM1) stations on either side of the main fault.

One alternative to be checked with our ITRF2000 velocity solution is to calculate velocities of all sites using No Net Rotation NUVEL-1A plate model (DeMets et al. 1994, McCarthy 1996).

Additionally, to better illustrate the deformation within the fault zone, strain rates of "eigenvalues" parameterization, the maximum extension ε_1, maximum compression ε_2 and its azimuth θ, and rotation Ω, were estimated for the whole network from the

ITRF2000 velocity solution (Feigl et al 1990, Yun 2000). The advantage of using the strain parameters is that they are almost invariant to the changes in the horizontal network scale and orientation (Vanícek and Krakiwsky 1986, Yun 2000).

3. Results and Discussions

The estimated velocities in ITRF2000 and by the model of NUVEL-1A are shown in Table 4 and Fig. 1. Our ITRF2000 horizontal velocity field components have uncertainties of about 3 mm/yr, almost two times larger than the present ones of velocity of IGS permanent stations in ITRF2000. It can be explained mainly by a rather small number of GPS data available, point centering by tripod, and type of antenna used in campaigns.

ITRF2000 and NUVEL-1A velocity sets were consistence -in direction at the most stations, but their velocity values were rather different. The velocity difference of maximum 10 mm/yr can be found at the sites in our network. This is not only due to definition of now available plate motion models that assumes rigid plates but also corresponds to conclusions of Michel et al. (2000, 2001) who reported that Sundaland, South-China, together with western and central parts of Indonesia form a stable block, which decouples from Eurasia and has faster east-southeastward movement than Eurasia itself.

Every estimated local horizontal velocity had the same uncertainty as the ITRF2000 solution. Most of these velocities were several millimeters/yr and at 95% confidence level, resulted in no displacement between

Table 4. Velocities estimated in ITRF2000 and by NUVEL-1A model

	ITRF2000		NUVEL-1A	
	VE (mm)	VN (mm)	VE (mm)	VN (mm)
DAEJ	28.1	-16.0	21.1	-14.2
SUWN	28.0	-15.2	21.1	-14.2
WUHN	32.8	-13.5	23.1	-12.0
NGA1	41.1	-9.0	23.7	-9.6
HAM1	35.4	-10.7	23.7	-9.6
TAU1	35.6	-11.1	23.6	-9.6
TAU2	35.2	-10.6	23.6	-9.6
DON1	36.9	-11.4	23.7	-9.5
LEM1	36.6	-10.5	23.7	-9.5
TAT1	35.3	-8.8	23.6	-9.5

the strands of the main fault, except NGA1 station, which gave a remarkable north-eastward, greater - than- 5 mm/yr velocity (solution with fixed stations: DON1 and LEM1). This result reconfirms the above-mentioned point of view of Michel et al. (2000, 2001), and favors the left-lateral strike-slip of the fault zone (Nguyen et al, 2001).

Concerning the whole network, the values of the most extensional, compressional, and rotational parameters are also insignificant and smaller than their standard errors. None of them were distinguishable from zero (no deformation) with 95% confidence.

However based on their direction we can interpret the estimated strain rates in terms of the fault's activity. Figure 2 shows estimated strain rates ε_1, ε_2 from ITRF2000 velocity solution. Azimuths of them correspond to maximum left-lateral simple shear on the sub-longitudinal striking LC-DBF. The maximum compression strain rate almost coincides with north-northwest trending compression at late stage of tectonic stress field of the LC-DBF which started, possibly, from Pliocene, 5 Ma ago (Nguyen et al. 2001, Burchfiel 2004). This result seems to be an interseismic deformation because no earthquake with magnitude larger than 5 happened within our geodetic network over the GPS measurements (2002-2004). Meanwhile, vertical velocity component was not precise enough for detecting reverse or normal faulting in a study area.

4. Conclusion

A series of GPS measurements for four epochs from 2002 to 2004 were used to detect the recent crustal movements in a local geodetic network spanning LC-DBF in Northwest of Vietnam. For crustal movement study cases, our ITRF2000 and local horizontal velocity solutions had only average precision, and any horizontal movement components smaller than 3 mm/yr could not be detected. On the basis of such level of precision and quantity of acquired data, we could only conclude that there were not much significant local displacement and deformation in the whole network at 95% confidence level between 2002 and 2004. In other words, present-day activities of the fault can be described as follows:

1) The LC-DBF system is most likely to be active in the present day as a left-lateral strike-slip fault as discussed by Nguyen et al. (2001), and Burchfiel (2004).

2) From a regional point of view, LC-DBF system on Sundaland, that is, Indochina, together with South -China are moving east-southeastward (Michel et al. 2000, 2001).

In order to improve the precision of velocity solution, more GPS campaigns must be carried out with use of an appropriate antenna and denser site distribution along the fault zone and its profile. With such velocity field, some models such as the simple elastic dislocation model can be applied for further interpretation of the recent activity of the LC-DBF.

Acknowledgments

References

1. Altamimi, Z., P. Sillard, and C. Boucher. (2002). *ITRF2000: A new release of the International Terrestrial Reference Frame for Earth Science Application*, J. Geophys. Res., Vol. 107, No. B10, 2214, doi: 10.1029/2001JB000561.
2. Becker, M., E. Reinhart, Soeb Bin Nordin, D. Angermann, G. Michel, and Ch. Reigber. (2000). *Improving the velocity field in South and South-East Asia: The third round of GEODYSSEA*, Earth Planets Space, 52, 721-726.
3. Burchfiel, B. C. (2004). *New Technology; New Geological Challenges*, Geological Society of America Today, v. 14, no. 2, p. 4-10, Feb.
4. DeMets, C., R. G. Gordon, D. F. Argus, and S. Stein. (1994). *Effect of Recent Revisions to the Geomagnetic Reversal Time Scale on Estimates of Current Plate Motions*, Geophys. Res. Let., 21, pp. 2,191-2,194.
5. Dong, D., T. A. Herring, and R. W. King. (1998). *Estimating regional deformation from a combination of space and terrestrial geodetic data*, Journal of Geodesy, 72, 200-214.

6. Duong Chi Cong, and K. L. Feigl. (1999). *Geodetic measurement of horizontal strain across the Red River fault near Thac Ba, Vietnam, 1963-1994*, Journal of Geodesy, 73, 298-310.

7. Feigl K. L., Duong Chi Cong, M. Becker, Tran Dinh To, K. Neumann, and Nguyen Quang Xuyen. (2003). *Insignificant horizontal strain across the Red River fault near Thac Ba, Vietnam from GPS measurements 1994-2000*, Geophysical Research Abstracts, Vol. 5, 04707, EGS-AGU-EUG Joint Assembly, Nice, France, 6-11 April 2003.

8. Feigl, K. L., R. W. King, and T. H. Jordan. (1990). *Geodetic measurement of tectonic deformation in the Santa Maria fold and thrust belt, California*, J. Geophys. Res., 95, 2,679-2,699.

9. Ha Minh Hoa, Tran Dinh To, Duong Chi Cong, Vy Quoc Hai, Nguyen Ngoc Lau, and others. (2003). *Application of GPS for Studying Crustal Movements and the First Results of Recent Displacement of Lai Chau-Dien Bien Fault Zone from Feb. 2002 to Feb. 2003*, Scientific Report, Hanoi, (*in Vietnamese*).

10. Herring, T. A. (2003). *GLOBK: Global Kalman filter VLBI and GPS analysis program, version 10.1*, MIT, Cambridge.

11. Holt, W. E., N. Chamot-Rooke, X. Le Pichon, A. J. Haines, B. Shen-Tu, and J. Ren. (2000). *Velocity field in Asia inferred from Quaternary fault slip rates and Global Positioning System observations*, J. Geophys. Res., Vol. 105, No. B8, 19,185-19,209, Aug. 10.

12. Lacassin, R., H. Maluski, P.H. Leloup, P. Tapponnier, Chaiyan Hinthong, Kanchit Siribhakdi, Saengathit Chuaviroj, and Adul Charoenravat. (1997). *Tertiary diachronic extrusion and deformation of western Indochina: Structural and 40Ar/39Ar evidence from NW Thailand*, J. Geophys. Res., vol. 102, no B5, 10,013-10,037, May 1997.

13. King, R. W., and Bock, Y. (2003). *Documentation for the GAMIT GPS analysis software, release 10.1*, MIT, Cambridge.

14. King, R. W., F. Shen, B. C. Burchfiel, L. H. Royden, E. Wang, Z. Chen, Y. Liu, X. Y. Zhang, J. X. Zhao, and Y. Li. (1997). *Geodetic measurement of crustal motion in southwest China*, Geology, Vol. 25, No. 2, pp. 179-182.

15. Larson, K. M., and D. C. Agnew. (1991) *Application of the Global Positioning System to crustal deformation measurement: 1. Precision and Accuracy*, J. Geophys. Res., 96, 16,547-16,565.

16. McCarthy, D. D. (1996). *IERS Technical Note 21*, U.S. Naval Observatory.

17. Michel, G. W., M. Becker, D. Angermann, Ch. Reigber, and E. Reinhart. (2000). *Crustal motion in E- and SE-Asia from GPS measurements*, Earth Planets Space, 52, 713-720.

18. Michel, G. W., Yue Qui Yu, Sheng Yuan Zhu, Ch. Reigber, M. Becker, E. Reinhart, W. Simons, B. Ambrosius, Ch. Vigny, N. Chamot-Rooke, X. Le Pichon, P. Morgan, and S. Matheussen. (2001). *Crustal motion and block behaviour in SE-Asia from GPS measurements*, Earth and Planetary Science Letters 178, 239-244.

19. Nguyen Ngoc Lau. (2002). *Relationship between satellite cut-off angle and elevation accuracy in GPS measurement technique*, Journal of Geodesy-Cartography, Vietnamese Society of Geodesy-Cartography, and Remote Sensing, No. 1/2002a, p. 35-47, Hanoi, (*in Vietnamese*).

20. Nguyen Ngoc Lau. (2002). *Role of atmospheric in high precision GPS data processing*, Journal of Geodesy-Cartography, Vietnamese Society of Geodesy-Cartography, and Remote Sensing, No. 2/2002b, p. 41-53, Hanoi, (*in Vietnamese*).

21. Nguyen Van Hung, and Hoang Quang Vinh. (2001). *Moving characteristics of the Lai Chau-Dien Bien Fault zone during Cenozoic*, Journal of GEOLOGY, Series B, No. 17-18/2001, p. 65-77, Hanoi.

22. Rothacher, M. and G. Mader. (1996). *Combination of antenna phase center offsets and variations: Antenna calibration set IGS_01*, http://www.aiub.unibe.ch.

23. Vanícek, P., and Krakiwsky, E. J. (1986). *Geodesy: The Concepts*, 2nd ed., 697 pp., North-Holland.

24. Wang, Q., Zhang P. Z., Freymueller J. T., Bilham R., Larson K. M., Lai X., You X., Niu Z., Wu J., Li Y., Liu J., Yang Z., and Chen Q. (2001). *Present-day crustal deformation in China constrained by Global Positioning System measurements*, Science, vol. 294, 19 Oct 2001, p. 574-577.

25. Wessel, P., and W. H. F. Smith, New, improved version of Generic Mapping Tools released, EOS. Trans. Amer. Geophys. U., vol. 79 (47), pp. 579, 1998.

26. Yun Hong Sic. (2000). *Application of Two Dimensional Filtering Technique for the Precision Calculation of Crustal Deformation Parameters*, Journal of Korean Society of Surveying, Geodesy, Photogrammetry, and Cartography, 4 v.018, n.001, pp. 75-83, (*in Korean*).

27. Yun Hong Sic, and Hwang Jin Sang. (2001). *Determination of Absolute Coordinates of Permanent GPS Site*, Journal of Korean Society of Surveying, Geodesy, Photogrammetry, and Cartography, 12 v.019, n.004, pp. 415-423, (*in Korean*).

28. Yun Hong Sic, and Hwang Jin Sang. (2002). *Comparison of Positioning Algorithms of GPS Data Processing Software for Analyzing the Ultra Long Baseline*, Journal of Korean Society of Civil Engineers (KSCE), Vol. 22, No. 3-D, pp. 571-582, (*in Korean*).

29. Zhang, Q., and W. Zhu. (2000). *The initial establishment of the tectonic block motion model of China from space geodetic data*, Chinese Science Bulletin, Vol. 45, No. 16, pp. 1523-1528.